Polarized Sorting of Rhodopsin on Post-Golgi Membranes in Frog Retinal Photoreceptor Cells

Dusanka Deretic and David S. Papermaster

Department of Pathology, University of Texas Health Science Center at San Antonio, San Antonio, Texas 78284-7750

Abstract. We have isolated a subcellular fraction of small vesicles (mean diameter, 300 nm) from frog photoreceptors, that accumulate newly synthesized rhodopsin with kinetics paralleling its appearance in post-Golgi membranes in vivo. This fraction is separated from other subcellular organelles including Golgi and plasma membranes and synaptic vesicles that are sorted to the opposite end of the photoreceptor cell. The vesicles have very low buoyant density in sucrose gradients (ρ = 1.09 g/ml), a relatively simple protein content and an orientation of rhodopsin expected of transport membranes. Reversible inhibition of transport by brefeldin A provides evidence that these vesicles are exocytic carriers. Specific immunoadsorption bound vesicles whose protein composition was indistinguishable from the membranes sedimented from the subcellular fraction. Some of these proteins may be cotransported with rhodopsin to the rod outer segment; others may be involved in vectorial transport.

COMPONENTS involved in the transport of membrane proteins through the Golgi stack have been studied extensively using a reconstituted cell-free system (Orci et. al., 1989; Melancon et. al., 1987). Developing such a system for studies of post-Golgi transport would require isolation of the subcellular compartments involved in sorting of membranes to various domains of the polarized cell (Rodriguez-Boulan and Nelson, 1989). This has been very difficult since vesicles and/or cisternae involved in the post-Golgi transport are transient intermediates and constitute a small fraction of the total population of smooth membranes of the cell. Transport vesicle isolation was facilitated in yeast, where temperature-sensitive mutants accumulate post-Golgi vesicles at the nonpermissive temperature (Walworth and Novick, 1987). Vesicles were also isolated from virus infected, unpolarized BHK cells (de Curtis and Simons, 1989) and mechanically perforated polarized MDCK cells (Bennet et al., 1988; Wandinger-Ness et al., 1990).

The highly polarized photoreceptor cells of the vertebrate retina have several advantages for the study of post-Golgi sorting of membrane proteins. These cells synthesize large amounts of a relatively simple membrane, mostly composed of a single membrane protein, rhodopsin, and sort opsin, the apoprotein of rhodopsin, and its associated proteins to a unique organelle, the rod outer segment (ROS)[1] (see Fig. 1). Rhodopsin constitutes ~85% of the ROS disk membrane protein and serves as the receptor to initiate visual excitation (Hall et al., 1969; Papermaster and Dreyer, 1974). Disk renewal (Fig. 1) requires addition of ~3 μm^2/min of ROS membranes in amphibians (Besharse, 1986). At the apex of the amphibian rod inner segment, small opsin-laden vesicles cluster beneath the base of the cilium (Besharse and Pfenninger, 1980; Peters et al., 1983). The *trans*-cisternae of the frog rod Golgi complex have been suggested to be a compartment for sorting of opsin and synaptophysin, proteins destined for opposite ends of the photoreceptor cells (Schmied and Holtzman, 1989); therefore opsin-bearing post-Golgi membranes should contain all the signals necessary for their proper sorting.

To isolate these membranes we have followed the kinetics of distribution of radiolabeled opsin in retinal subcellular fractions that have been separated on linear sucrose density gradients. Similar gradients were used for the separation of the vesicles carrying apical and basolateral proteins of the rat hepatocyte plasma membrane (Bartles et al., 1987) and for the sedimentation of the transport vesicles released from perforated MDCK cells (Bennet et al., 1988). This strategy generated a subcellular fraction with a very low buoyant density that accumulates newly synthesized opsin after it has been chased from the Golgi. We have successfully inhibited this accumulation using brefeldin A (BFA), a drug that inhibits protein transport by disrupting the dynamic membrane pathway between the ER and Golgi (Lippincott-Schwartz et al., 1989, 1990; Ulmer and Palade, 1989). BFA has been shown to have a similar effect on photoreceptor cells, inhibiting arrival of the newly synthesized proteins, but not lipids, to the rod outer segments (Fliesler, S. J., and R. K. Keller. 1989. *J. Cell Biol.* 109 [No. 4, Pt. 2]:206a[Abstr.]).

The composition, the orientation of opsin on the vesicles that we have isolated and the cell's response to BFA, indicate that these vesicles have properties expected of post-Golgi membranes that are transporting proteins destined for the ROS.

1. *Abbreviations used in this paper*: BFA, brefeldin A; ROS, rod outer segment.

Materials and Methods

Frogs, *Rana berlandieri*, (100–250 g) purchased from Rana Co. (Brownsville, TX), were maintained in a 12-h light/dark cycle and fed live crickets. MEM Select-Amine Kit was from Gibco Laboratories (Grand Island, NY), protease inhibitors from Sigma Chemical Co. (St. Louis, MO), BFA from Epicentre Technologies (Madison, WI), [^{35}S]methionine (1,000 Ci/mmol) and UDP-[^{3}H]galactose (10.5 Ci/mmol) from New England Nuclear (Boston, MA), hexyl-β-D-glucopyranoside and thermolysin from Calbiochem-Behring Corp. (La Jolla, CA), Eupergit-C1Z beads (manufactured by Rohm Pharma, Weitezstadt, Germany) from Accurate Chemical & Scientific Corp. (Westbury, NY), peroxidase conjugated anti-mouse and anti-rabbit IgG from Kirkegaard and Perry (Gaithersburg, MD), rabbit anti-mouse IgG from Jackson Immuno Research Laboratories, Inc. (Avondale, PA), goat anti-rabbit IgG conjugated to 10-nm gold from Janssen Life Sciences Products (Piscataway, NJ), and Screen Type kit from Boehringer Mannheim Diagnostics, Inc. (Houston, TX).

Several antibodies were kindly provided for this study: monoclonal antibody E to frog rhodopsin's NH_2 terminus by Dr. H. E. Hamm (University of Illinois, Chicago, IL); mAb 1D4 anti-bovine rhodopsin COOH-terminal by Dr. R. Molday (University of British Columbia, Vancouver, BC); antiserum to frog arrestin ("48K" protein) by Dr. N. Mangini (University of Illinois); anti-Na,K-ATPase by Dr. R. Mercer (Washington University, St. Louis, MO); and anti-synaptophysin by Dr. F. Valtorta (University of Milan, Milan, Italy), respectively.

In Vitro Incorporation of [^{35}S]Methionine and Retinal Subcellular Fractionation

All experiments were conducted under dim red light: frogs were returned to darkness (to facilitate retinal isolation) 2 h before the time of light offset. Preliminary experiments indicated that protein synthesis was maximal in the late afternoon. Frog eyecups or isolated retinas were incubated in oxygenated medium which was prepared as follows. Amino acids and vitamins were reconstituted from the MEM Select-Amine Kit to final concentrations described by Wolf and Quimby (1964), cold methionine was omitted except during the chase. To this medium salts were added according to the in vitro incubation medium described by Greenberger and Besharse (1983). In the experiments involving BFA, the drug was added from a 5 mg/ml solution in methanol to reach a final concentration of 5 μg/ml (Ulmer and Palade, 1989).

Seven eyecups or retinas were incubated in 15 ml of media at 20°C, and [^{35}S]methionine (25 μCi per retina) was added. No differences were observed with either preparation. After each incorporation, retinas were isolated from eyecups and ROS were purified on a step sucrose gradient as described by Papermaster and Dreyer (1974) with the addition of protease inhibitors: 10 μg/ml antipain, 2 μM leupeptin, and 100 KIU/ml aprotinin. Retinal pellets were rehomogenized as described by Papermaster et al. (1975). Supernatants (3 ml) were overlaid on 10 ml linear 20–39% (wt/wt) sucrose gradients containing protease inhibitors as above in 10 mM Tris-acetate pH 7.4 and 1 mM $MgCl_2$, above a 0.5-ml cushion of 49% (wt/wt) sucrose in the same buffer (Dunn and Hubbard, 1984). The gradients were prepared using a Buchler Auto Densi-Flow fractionator (Buchler Instrument Inc., Fort Lee, NJ). After centrifugation at 100,000 g_{av} for 13 h in a rotor (SW40; Beckman Instruments, Inc., Palo Alto, CA) at 4°C, 0.9-ml fractions were reproducibly collected from the top of the gradient using the same fractionator.

The refractive index and galactosyl-transferase activity of each fraction was determined using a small aliquot and the remainder was diluted with 10 mM Tris pH 7.4 and centrifuged at 40,000 rpm for 40 min in a rotor (SW40; Beckman Instruments, Inc.). Pellets were resuspended in 10 mM Tris pH 7.4 and aliquoted for determination of protein concentration, radioactivity, and for analysis by SDS-PAGE. Protein samples were solubilized in 50% hexyl-β-D-glucopyranoside (final concentration 8%) and protein concentrations were determined using the Bradford protein assay modified for membrane proteins (Fanger, 1987). Samples were resuspended in Optifluor and radioactivity was determined in a scintillation counter (LS7000; Beckman Instruments, Inc.). Channels ratios were compared to determine the relative quenching and varied little. Galactosyl-transferase activity was measured as described by Bartles et al. (1987).

SDS-PAGE, Autoradiography, and Immunoblotting

Membranes that were pelleted at 40,000 rpm for 40 min in a rotor (SW40; Beckman Instruments, Inc.) after dilution of different retinal fractions were solubilized and separated on 10% SDS-PAGE according to Laemmli (1970). Gels were stained and impregnated with 1 M Na-salicylate for 1 h, dried, and autoradiographed repeatedly for various times at −70°C using Kodak X-Omat film with intensifying screens. To obtain autoradiographs within linear range of the film, exposure times in the different experiments varied greatly. Autoradiographs were scanned with the laser densitometer (LKB Instruments, Inc., Gaithersburg, MD). SDS-PAGE gels were blotted onto Immobilon-P membranes according to Matsudaira (1987). Blots were incubated in 5% nonfat dry milk, 1% BSA, and 0.1% Tween 20 in TBS (20 mM Tris pH 7.5, 500 mM NaCl) for 1 h in order to reduce nonspecific protein binding. Antibodies were diluted to 1 μg/ml in TTBS (TBS containing 0.05% Tween 20) and incubated for 2 h at 20°C. After three washes in TBS and TTBS, immunoblots were incubated for 1 h in peroxidase-conjugated anti-mouse (or anti-rabbit) IgG diluted 1:2,000 and bound antibodies were detected as described in Deretic and Hamm (1987).

Thermolysin Digestion of ROS and Fraction 5 Membranes

Membranes were digested with thermolysin as described by Kühn et al. (1982) and Hargrave et al. (1987). Thermolysin was added to a final ratio of 4 μg of enzyme/25 μg of protein in a total volume of 80 μl containing 10 mM Tris acetate, pH 7.4 and 4 mM $CaCl_2$. After 1 h at 20°C, digestion was stopped with 0.2 M EDTA and digestion products were analyzed by SDS-PAGE, immunoblotting, and autoradiography.

Preparation of mAb 11D5

A BALB/c mouse was injected intraperitoneally with 50 μg of fraction 5 membranes and boosted with the same membranes mixed with excess mAb E to the NH_2-terminal domain of rhodopsin (Adamus et al., 1985) and mAb 1D4 to the COOH-terminal domain (MacKenzie et al., 1984). Antibody-producing hybridomas were obtained by the method of Kohler and Milstein (1975). ELISA plates were coated with fraction 5 proteins, 25 ng/well; antibody-producing hybridomas were detected using peroxidase-conjugated anti-mouse IgG and isotyped using the Screen Type kit. mAb 11D5 belongs to the IgG1 subclass. Hybridomas producing this antibody were subcloned twice by the method of limiting dilution. Antibody was purified from ascites fluid on a protein A–Sepharose 4B affinity column as described by Ey et al. (1981). Specificity of the antibody was tested by immunoblotting (as described above).

Immunoisolation of the Vesicles

Immunoisolation using mAb 11D5 and murine IgG1 was performed as described by Burger et al. (1989). The final concentration of bound antibody or IgG1 was ~7 μg/mg of beads. Beads were blocked for 1 h with 5% nonfat dry milk and 1% BSA in PBS in order to reduce nonspecific binding (which varied between 5 and 15%). The retinas were radiolabeled by 90 min of incubation with [^{35}S]methionine and 2 h of cold chase. Coated beads (2.5 mg) were incubated with 20 μg of fraction 5 (equivalent to membranes sedimented at 40,000 rpm from four retinas), for 2 h at 4°C, either after pelleting or directly from the sucrose gradient fraction. After several washes with 0.25 M sucrose containing protease inhibitors (as described above in the homogenizing buffer), each sample was divided in two portions and half of the immunobeads, with bound organelles, was resuspended in 150 mM NaCl, 10 mM Tris pH 7.4, containing 2% SDS and protease inhibitors (as described above), and analyzed by SDS-PAGE. The other half was fixed and processed for EM analysis as described below.

Electron Microscopy

After in vitro incubation with [^{35}S]methionine in the presence or absence of BFA, retinas were fixed in 4% formaldehyde and 1% glutaraldehyde in 0.12 M cacodylate buffer pH 7.5 for 1 h at 20°C, postfixed in OsO_4 and embedded in Epon.

Membranes from the sucrose gradient fractions were pelleted for 1 h at 50,000 rpm in a rotor (SW50.1; Beckman Instruments, Inc.) with adaptors to obtain a small pellet. Pellets were fixed with 2% glutaraldehyde in 120 mM cacodylate pH 7.4 containing 3% sucrose, for 30 min on ice, postfixed with OsO_4, stained with uranyl acetate, and embedded in 2% agarose by a modified procedure of De Camilli et al. (1983). Blocks of membranes in agarose were formed in Eppendorf microcentrifuge tubes (Brinkmann Instruments Co., Westbury, CT) dehydrated in ethanol and embedded in Epon.

Immunoisolated vesicles, attached to the immunobeads, were fixed in 3% glutaraldehyde in 100 mM cacodylate, pH 7.4 containing 7.5% sucrose,

for 1 h on ice, rinsed, resuspended in the same buffer, and mixed with an equal volume of 2% agarose. Small blocks were formed, postfixed with OsO_4, dehydrated, and embedded in Epon.

Frog retinas were embedded in LR gold and labeled with mAb 11D5 according to the procedure of Berryman and Rodewald (1990), except that postfixation with OsO_4 was omitted. Bound mAb 11D5 was detected by rabbit anti-mouse IgG and goat anti-rabbit IgG conjugated to 10-nm gold. Thin sections were stained with uranyl acetate and lead citrate. All thin sections were examined in a Philips 301 electron microscope.

To measure the average vesicle diameter, pellets of retinal subcellular fractions obtained from one experiment were sectioned parallel to the longitudinal axis of sedimentation and electron micrographs (×16,500) were obtained by random sampling. A point counting grid was overlaid randomly on 10 images; 10 vesicles were chosen at intersections of the grid from each image and were measured with a graded series of circles (Weibel, 1979). Review of sections of retinal fractions from multiple experiments indicated that the sample chosen for quantitative analysis was representative.

Results

Newly Synthesized Opsin Accumulates in Vesicles of Low Buoyant Density with a Kinetics that Parallels Its Appearance in Post-Golgi Membranes In Vivo

Movement of newly synthesized opsin through the subcellular compartments of the retinal rods was followed by the pulse-chase experiments. [^{35}S]Methionine incorporation times were chosen according to the in vivo studies schematically presented in Fig. 1. After various periods of incubation, retinas were isolated from the eyecups. ROS were removed, the remaining radiolabeled membranes were separated on linear 20–39% sucrose gradients, pelleted, and specific activity of each gradient fraction was determined (Fig. 2).

After 30 min of [^{35}S]methionine incorporation, the specific activity of sedimentable protein is highest in fraction 14 (ρ = 1.19 g/ml), which corresponds to the density of ER membranes in sucrose (Balch et al., 1984). By 90 min of incubation, newly synthesized proteins distribute predominantly in fractions which also contain galactosyl-transferase activity, a marker for Golgi membranes (ρ = 1.2–1.16 g/ml).

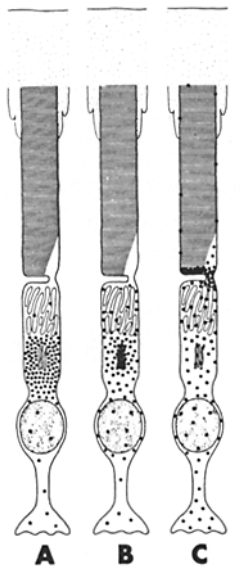

Figure 1. Diagram of the kinetics of synthesis and transport of radiolabeled proteins in frog retinal rods in vivo. (Modified from Young, 1976, with permission.) (*A*) Shortly after exposure to radiolabeled amino acids, the RER becomes highly labeled in the rod inner segment (*RIS*). (*B*) After 30–60 min, the Golgi apparatus (*G*) in the inner segment becomes the most labeled site. (*C*) After an additional 1–2 h, newly synthesized proteins are mostly transported vectorially to the base of the rod outer segment (*ROS*), although some are transported to the synapse (*SYN*) at the opposite end of the cell. During subsequent weeks, the basal disks are displaced from below by addition of new disks until they reach the tip of the ROS. There the membranes are shed, engulfed by the adjacent retinal pigment epithelium (*PE*), and destroyed.

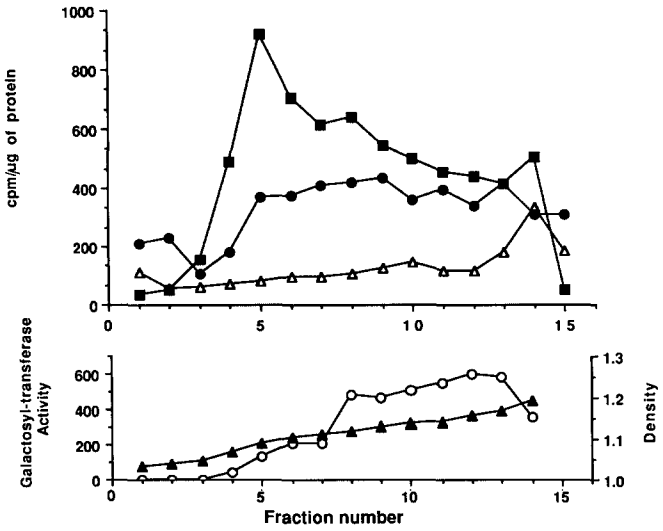

Figure 2. Distribution of radiolabeled retinal membrane proteins separated on linear sucrose density gradients after various periods of radiolabeled amino acid incorporation. Isolated frog eyecups were incubated in the presence of [^{35}S]methionine. After homogenization and differential sedimentation, retinal subcellular fractions were separated on linear sucrose density gradients (*bottom, solid triangles*). The galactosyl-transferase activity of each fraction was determined (*bottom, open circles*), as well as specific activity of pelleted membranes (*top*). The incubations were for: (*open triangles*) 30 min; (*solid circles*) 90 min; (*solid squares*) 90 min and 2 h of "cold" chase.

When 90 min of incorporation is followed by 2 h of cold chase, fraction 5, with a very low buoyant density (ρ = 1.09 g/ml), becomes highly labeled. This low density fraction has the highest specific activity at this time, and yet it contains only 0.03% of the total protein isolated from the retinal homogenate (not including the ROS separated in the first step of the fractionation).

The population of radiolabeled membrane proteins of fraction 5 is relatively simple when compared to the other subcellular fractions. A representative SDS-PAGE gel of all of the fractions is shown in Fig. 3 *A* and its autoradiograph in Fig. 3 *B*. Fractions 9–14 appear relatively similar in their composition, their total protein content, and the relative abundance of opsin, which is a minor protein in these fractions. Fractions 7 and 8 have a low protein content, but their relative opsin content is higher, partly because small amounts of residual ROS are incompletely separated during the first step of the fractionation and cosediment with these two fractions (ρ = 1.12–1.13 g/ml). Fraction 5 membranes contain fewer proteins and some of them are enriched, especially polypeptides of 50 and 20 kD. The opsin content in this fraction is comparable to other retinal fractions (except 7 and 8) and its apparent molecular weight is the same as the mature rhodopsin isolated from ROS (shown in the last lane). The gel shown in Fig. 3 *A*, exposed to prolonged autoradiography (Fig. 3 *B*) reveals that proteins enriched in fraction 5 are also radiolabeled after 90 min of isotope incorporation followed by 2 h of cold chase. However, opsin is the major radiolabeled protein in all of the subcellular fractions.

To quantitate the amount of [^{35}S]methionine incorporated into opsin after various times of incubation, less exposed au-

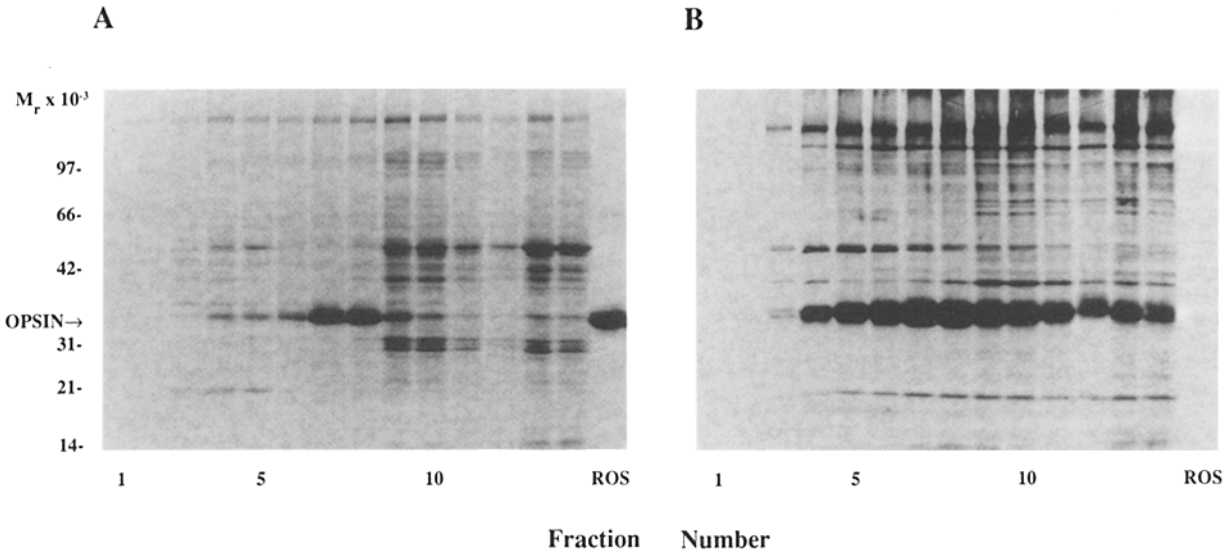

Figure 3. Radiolabeled retinal proteins separated by SDS-PAGE. Membranes were pelleted from retinal subcellular fractions of the linear sucrose gradient after 90 min of [^{35}S]methionine incorporation followed by 2 h of cold chase, and separated by SDS-PAGE on a 10% gel. The gel was stained with Coomassie blue (*A*), dried, and autoradiographed for 2 d at −70°C (*B*). Aliquots in each lane contained the membranes isolated from six retinas. The ROS aliquot equals 0.2 retinas. Migration of molecular weight standards is indicated, as is the migration of opsin, which is the major radiolabeled protein synthesized by the retina. This gel was exposed for a long period so that its autoradiograph would be useful to demonstrate minor radiolabeled proteins. The opsin region is, therefore, greatly overexposed. The autoradiographs of this same gel that are generated after shorter exposure resemble that which is shown in Fig. 4 *A* (90 min + chase), namely fraction 5 contains the greatest amount of radiolabeled opsin.

toradiographs of the opsin region of the gels at each incubation condition were compared (Fig. 4, *A* and *B*). After 30 min of isotope incorporation, radiolabeled opsin is found predominantly in the heavy fractions of the gradient (fractions 8–14). Electrophoretic migration of the newly synthesized opsin in fractions 13 and 14 is slower, suggesting that higher molecular weight forms of opsin predominate in those fractions, probably with untrimmed oligosaccharides, in contrast to mature opsin which has two unusually short hexasaccharide chains (Fukuda et al., 1979; Liang et al., 1979). During the subsequent course of protein synthesis in the presence of [^{35}S]methionine, the greatest amount of radiolabeled opsin is found in the Golgi-enriched fractions, and it has the same mobility as mature rhodopsin in ROS.

Only after the chase, when the Golgi apparatus is relatively depleted, does radiolabeled opsin predominantly accumulate in fraction 5 (Fig. 4, *A* and *B*). This result suggests that fraction 5 contains post-Golgi membranes that are transporting opsin vectorially to the outer segment. Further evidence for this functional assignment comes from the kinetics of appearance of newly synthesized opsin in the outer segments as fraction 5 becomes highly labeled. Fig. 4 *C* shows that after 90 min of incubation with the labeled precursor followed by two hours of cold chase, radiolabeled opsin begins to be recovered in ROS fractions. Thus newly synthesized opsin arrives in ROS fractions after in vitro isotope incorporation at intervals that parallel prior in vivo studies of transport of radiolabeled proteins in rods, schematically presented in Fig. 1 (Young and Droz, 1968; Hall et al., 1969; Papermaster et al., 1975, 1985, 1986).

Low Buoyant Density Vesicles Carrying Newly Synthesized Opsin Are Separated from Synaptic Vesicles As Well As from Vesiculated Plasma Membranes

Opsin and synaptophysin, a synaptic membrane protein, are sorted to the opposite ends of the photoreceptor cells. Sorting of these proteins occurs from the Golgi apparatus, since they have been colocalized in the *trans*-Golgi cisternae of the frog rods, but not on the same transport vesicles (Schmied and Holtzman, 1989). Opsin bearing vesicles therefore, should not contain synaptophysin. To localize this protein we have reacted blots of retinal subcellular fractions with an antibody to frog synaptophysin (Valtorta et al., 1988). Membranes containing synaptophysin sediment in fractions 6–11 and represent only a minor contaminant (or component) of fraction 5 (Fig. 5, *bottom*). Reaction of the same blot with antibody to soluble cytosolic protein, arrestin (48K) (Mangini and Pepperberg, 1988), reveals that this protein is found predominantly in fraction 3, indicating that unbound cytosolic proteins remain mostly on the top of the gradient and are not found significantly in fraction 5. This suggests that proteins found in fraction 5 that are not sedimentable in the 40,000 rpm pellet (see Fig. 11 *B*), may be peripherally associated with the membranes.

Immunoblots of retinal subcellular fractions with an antibody to Na,K-ATPase (Fig. 5, *top*), an enzyme localized exclusively in the plasma membrane of the photoreceptor inner segment (Schneider and Kraig, 1990; Schneider et al., 1991), revealed that majority of the plasma membrane-derived vesicles sediments in heavier fractions 9–11, corre-

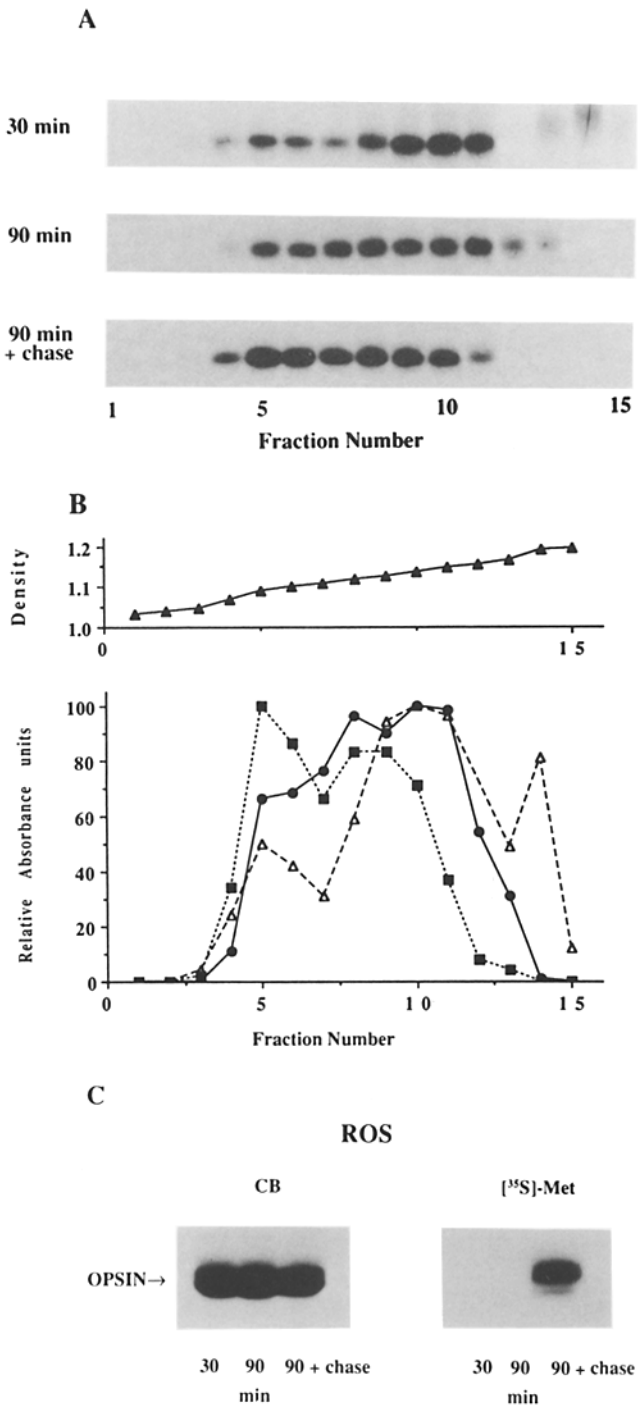

Figure 4. The maximum level of newly synthesized opsin shifts to the fraction of light vesicles (fraction 5) after the cold chase, at the same time that radiolabeled opsin appears, at low levels, in the ROS. (*A*) Opsin region of the autoradiographs. Membranes were pelleted from retinal subcellular fractions as indicated and separated on 10% SDS-PAGE. Aliquots equal to membranes from three retinas were separated in each lane. Gels were dried and autoradiographed. The autoradiographs chosen for this figure were exposed at −70°C as follows: 30-min incubation, 6 d; 90-min incubation, 2 d; 90-min incubation and 2 h of cold chase, 1 d so that incorporation into the opsin band could be quantitated. Various exposure times were necessary for densitometric quantitation since the specific activity of fraction 5 proteins increases >10-fold between 30 min of incorporation and 90 min + 2-h chase (see Fig. 2). Using this approach, only the fractions that contain the greatest amount of radiolabeled opsin at a given time are apparently radiolabeled. Although radiolabeled opsin persists in fractions 12–14 after 90 min of incorporation and even after 2 h chase, it can be detected only after prolonged autoradiography as shown in Fig. 3 *B*, since its proportional specific activity relative to lighter fractions is small. (*B*) Results of laser densitometry expressed as the relative percentage of maximal density of the fraction containing the greatest amount of labeled opsin. (*Open triangles*) 30 min; (*solid circles*) 90 min; (*solid squares*) 90 min and 2 h of cold chase. (*C*) ROS were sheared off the retinas at the indicated time points, fractionated on discontinuous sucrose density gradients, and aliquots equal to 0.7 retinas were electrophoresed on a 10% SDS-PAGE gel. The gel was stained with Coomassie blue (*CB*), dried, and autoradiographed for 6 d at −70°C (*[35S]-Met*).

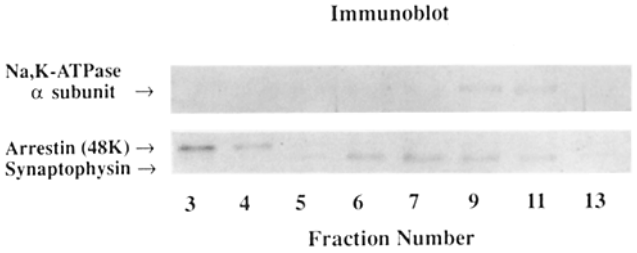

Figure 5. A synaptic membrane protein (synaptophysin), a plasma membrane protein of the inner segment, (Na,K-ATPase), and soluble protein (arrestin) are virtually absent from fraction 5. Both synaptophysin and Na,K-ATPase are found in more dense fractions while arrestin sediments in fractions of lesser density than fraction 5. Retinal proteins separated on the SDS-PAGE gel were blotted onto Immobilon-P membranes and immunoreactivity with different antibodies was determined, as indicated on the figure. The immunoblot shown on the lower panel was first incubated with antiserum to arrestin, developed to reveal bound peroxidase activity, incubated with antiserum to synaptophysin, and developed again.

sponding to the densities of plasma membranes previously described in other cells (Dunn and Hubbard, 1984).

Post-Golgi membranes carrying newly synthesized opsin are therefore separated from cytosol, vesiculated plasma membranes and the synaptic vesicles of the opposite end of the rod cell on the sucrose density gradients we used.

Vesicles Accumulating Newly Synthesized Opsin Are Exocytic Carriers

We investigated the source of the vesicles further by use of the fungal antibiotic BFA which reversibly blocks transport of newly synthesized membrane proteins by inducing membrane flow from the Golgi back to the rough endoplasmic reticulum (Ulmer and Palade, 1989; Lippincott-Schwartz et al., 1989, 1990) in many cells, including photoreceptors (Fliesler and Keller, 1989), and does not inhibit endocytosis (Misumi et al., 1986). We included BFA in the incubation media of isolated retinas for various time periods of pulse-chase experiments and followed intracellular opsin transport. Electron micrographs of BFA-treated retinas reveal the disruption of the Golgi apparatus and redistribution of ER and smooth membrane elements in the rod inner segment. These results completely parallel the results described earlier by S. J. Fliesler and R. K. Keller (1989. *J. Cell Biol.* 109

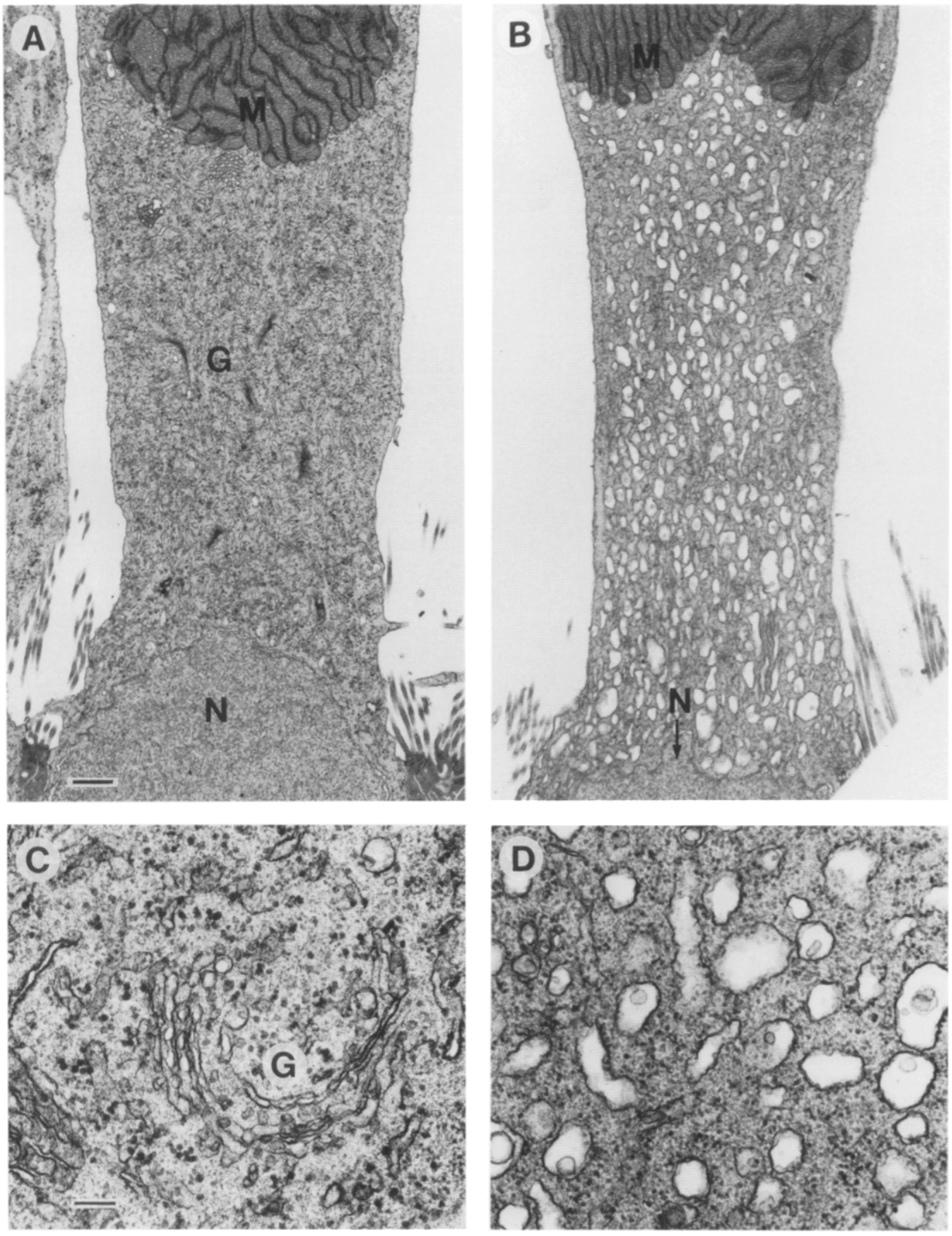

Figure 6. Electron microscopy of BFA-treated retinas demonstrates profound disruption and vesiculation of inner segment Golgi and RER membranes. Each retina was studied with randomly selected longitudinal sections. (*A* and *C*) The control retina, incubated without BFA has orderly, longitudinally stacked Golgi elements (*G*) comparable to the appearance of the inner segment in vivo. (*B* and *D*) Incubation of retinas in 5 μg/ml of BFA for 4.5 h shifts Golgi elements into a merged cisternal network. Stacked Golgi elements are not apparent. *N*, nucleus; *M*, mitochondria. Bars: (*A* and *B*) 1 μm; (*C* and *D*) 0.2 μm.

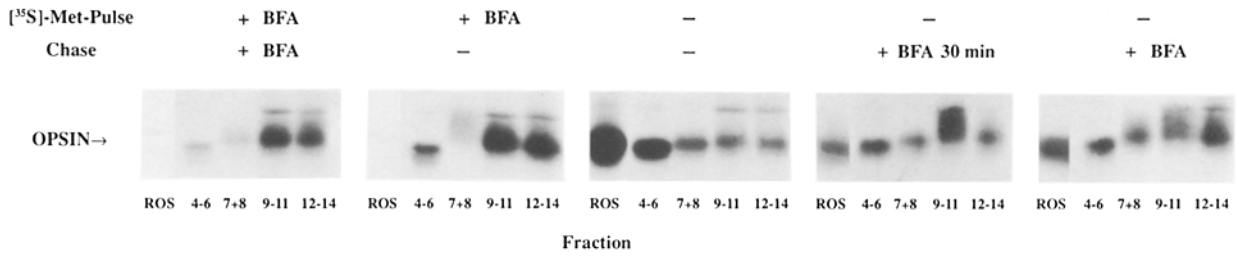

Figure 7. Delivery of radiolabeled opsin to the ROS and post-Golgi vesicles is inhibited by BFA; after removal of the drug during the chase, newly synthesized opsin enters fraction 5 before its delivery to the ROS. Post-Golgi transport is not inhibited by BFA added only during the chase. First and second panels: retinas were preincubated for 50 min with BFA and further incubated with BFA during 90 min of [^{35}S]methionine incorporation; BFA was also present (first panel) or absent (second panel) during a 2-h chase. Third panel (control): 90-min pulse/2-h chase experiment was performed in the absence of BFA. Fourth and fifth panels: retinas were labeled for 90 min with [^{35}S]methionine and BFA was added only during the cold chase which lasted either 30 min (fourth panel) or 2 h (fifth panel). Membranes were pelleted from the ROS and pooled retinal subcellular fractions and were separated on a 10% SDS-PAGE gel. Autoradiographs were exposed at −70°C for 5 d (*ROS*), or 4 h (pooled gradient fractions). Aliquots in each ROS sample equal 0.5 retinas and aliquots from each pooled fraction are equivalent to 2 retinas.

[No. 4, Pt. 2]:206a[Abstr.]). Control retinal rods all contain stacked Golgi membranes (Fig. 6, *A* and *C*). No intact Golgi membrane is seen in cells treated with BFA (Fig. 6, *B* and *D*).

To study the effect of constant exposure to BFA on opsin transport, we preincubated retinas for 50 min in the presence of 5 μg/ml of the drug before addition of [^{35}S]methionine, continued the 90-min pulse–2-h chase experiment in the presence of BFA, and monitored intracellular opsin transport by subcellular fractionation. The total amount of incorporated radioactivity is the same as in the control samples (data not shown), therefore BFA has no significant effect on protein synthesis in the retina. The effects of BFA on delivery of radiolabeled opsin to the ROS and its distribution in the pooled gradient fractions were assessed by SDS-PAGE and autoradiography (Fig. 7). In the presence of BFA, virtually no newly synthesized opsin is found in the outer segment fractions (Fig. 7, *ROS*, first panel), even if the drug is removed during the chase (*ROS*, second panel). 2 h of chase after removal of BFA are insufficient to restore post-Golgi transport and insertion of opsin into newly formed disks. Distribution of radiolabeled opsin in the pooled subcellular fractions of drug treated retinas changes dramatically compared to the control (Fig. 7, first and third panel). Only a very small amount of newly synthesized opsin collects in fractions 4–6 and the majority shifts to heavy fractions (9–14). The fraction 4–6 pool begins to regain its radiolabeled content when BFA is removed during the chase (Fig. 7, second panel), before newly synthesized opsin reaches the outer segments.

If BFA is introduced only during a 30-min chase, small amounts of labeled opsin appear in the outer segments and even more accumulates after 2 h of chase in the presence of BFA (Fig. 7, *ROS*, fourth and fifth panel). Although the fraction 4–6 pool has a lower content of radiolabeled opsin in the presence of BFA during the chase, (Fig. 7, fourth and fifth panel) compared to the control (third panel), those fractions still contain a considerable post-Golgi pool of radiolabeled vesicles that form during 90 min of isotope incorporation without BFA. Therefore, those radiolabeled membranes that have already escaped the Golgi apparatus after 90 min of incubation can complete their journey to the outer segment unimpeded by the drug.

The effects of BFA in these transport studies further support our interpretation that pooled fractions 4–6 contain a compartment that acquires newly synthesized opsin only after it has passed through the Golgi region but before it reaches the outer segments.

Isolated Post-Golgi Vesicles Are Relatively Homogeneous

Fraction 5 was compared morphologically to the other fractions separated on the sucrose gradient. Fig. 8 shows typical electron micrographs of thin sections through the pellets obtained from fraction 5 (*A*) and fractions 7, 9, and 11 (*B*, *C*, and *D*, respectively). Fraction 5 contains numerous small vesicles varying from 50 to 350 nm and very little contamination with other morphologically distinguishable subcellular organelles. By contrast, both lower density (fraction 3, data not shown), and higher density fractions (7, 9, and 11) are morphologically very heterogeneous. Besides vesicle-like structures they also contain membranous sheets, stacks of ROS disks, broken mitochondria, Golgi fragments, and ER membranes. These major differences in the appearance of the fractions are also reflected in their protein composition, as shown in Fig. 3 *A*. Therefore, fraction 5 is enriched in a relatively homogeneous population of vesicles with similar properties including, buoyant density, size, morphology, and rather simple protein content.

Opsin in Isolated Post-Golgi Vesicles Has an Orientation Comparable to the Transport Vesicles In Vivo

In the vesicles clustered beneath the connecting cilium in situ, opsin is embedded in the lipid bilayer with the same orientation as in the ROS disks, with the NH_2 terminus exposed on the inside of the vesicle surface (Defoe and Besharse, 1985). By analogy to the ROS disks, this orientation would place opsin's COOH-terminal domain on the cytoplasmic surface of the vesicle. We tested the topology of the opsin in the vesicles of fraction 5 by determining the susceptibility of opsin in the membrane to limited thermolytic digestion. Thermolysin cleaves bovine opsin's carboxy-terminal peptide 337–348 in the initial stages, and with more extensive proteolysis

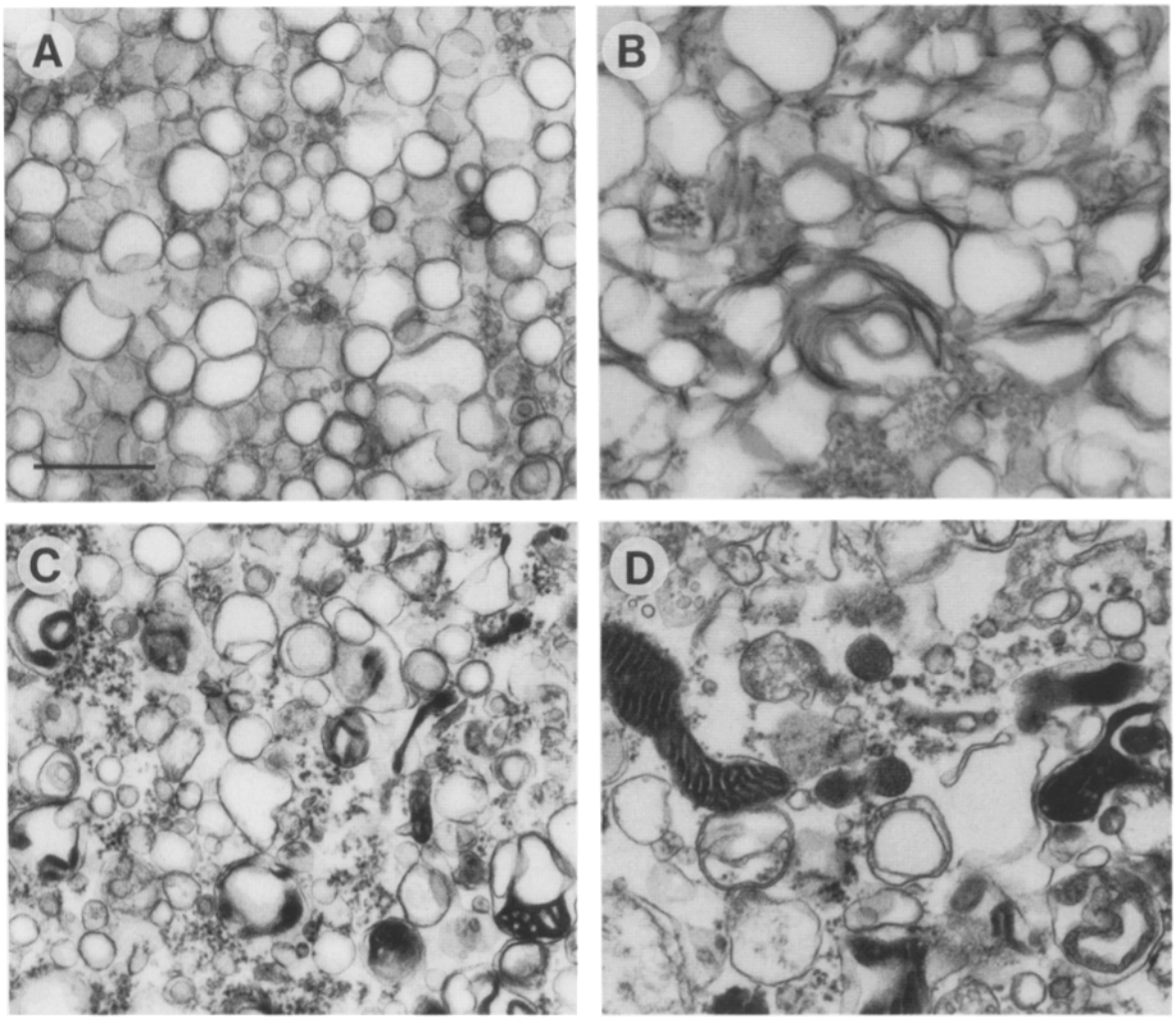

Figure 8. Electron micrographs of representative fractions from the linear sucrose gradient. (*A*) Fraction 5. Small vesicles (~300 nm) predominate; Large (~1 μm) and very small (<50 nm) vesicles are a minor fraction. (*B*) Fraction 7. ROS membranes in the form of apposed membrane disk fragments and large vesicles (1–3 μm) are the major component. (*C*) Fraction 9. Smooth membranes predominate in this very heterogeneous fraction. Occasional Golgi-like profiles are seen, but most of the membranes are not distinctive. (*D*) Fraction 11. This heterogeneous fraction contains abundant broken mitochondria, dark vesicles (possibly fragmented melanosomes from pigment epithelium), multivesicular bodies, and rough and smooth membranes. Bar, 0.5 μm.

of membrane-bound rhodopsin in ROS disks, yields an F1 fragment (containing the NH_2-terminal two-thirds of the protein) and an F2 fragment (containing the COOH-terminal one-third), from which 4, 12, or 21 COOH-terminal amino acids are removed by digestion at three additional sites (Hargrave et al., 1987). This is schematically shown in the diagram in Fig. 9.

We detected the reaction products of thermolytic digestion of frog ROS and fraction 5 membranes on immunoblots with mAb E, which is one of the antibodies that binds to opsin's NH_2-terminal described by Adamus et al. (1985) and mAb 11D5 (which reacts with opsin's COOH-terminal domain as described below). The results are shown in Fig. 9. Reactivity of immunoblots of ROS membranes or fraction 5 vesicle membranes with mAb 11D5 is largely lost after digestion with thermolysin. mAb E detects native opsin, its dimer (69 kD), as well as two smaller digestion products: ~32 kD (consistent with the loss of 12 COOH-terminal amino acids) and ~26 kD (comparable to bovine opsin fragment F1). Therefore, the carboxy-terminal domain of opsin is susceptible to the proteolytic action of thermolysin, consistent with its exposure at the cytoplasmic surface of the vesicle. There is more undigested opsin remaining in the fraction 5 digestion product than in the digested ROS, which may suggest that there is a small proportion of inside-out vesicles in this fraction. However, the relative abundance of the F1 fragment in the digestion products suggests that proteolysis is slower with fraction 5 membranes. Conformational change of rhodopsin in bovine ROS upon bleaching has been shown to influence the kinetics of digestion (Kühn et al., 1982), and our results may simply reflect a different conformation of opsin in fraction 5 compared to ROS.

Specificity of mAb 11D5

mAb 11D5 was generated by immunization of a BALB/c mouse with fraction 5 membranes. This antibody detects opsin in the immunoblots of fraction 5 and ROS membranes as

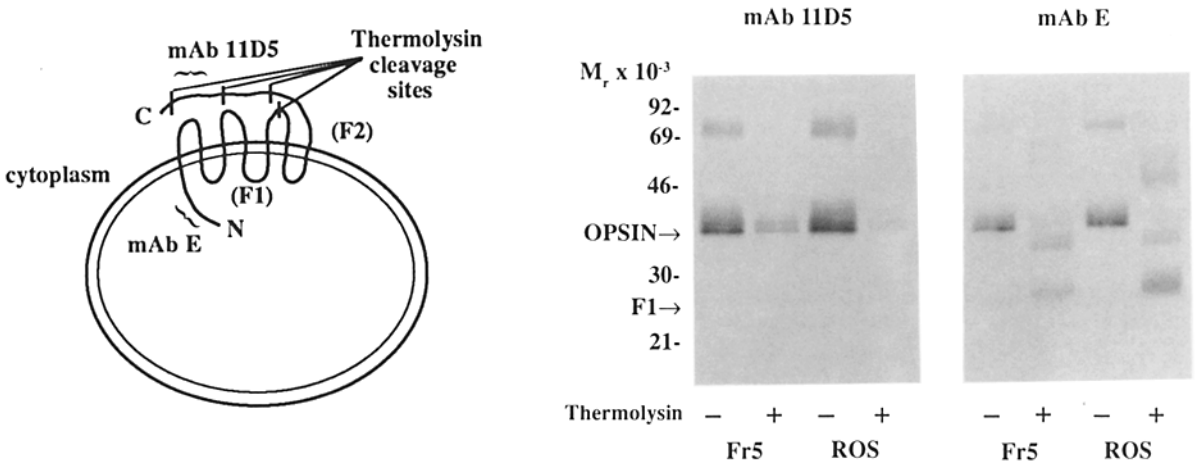

Figure 9. Topology of opsin in ROS and fraction 5 vesicles probed by thermolysin digestion and immunoblotting with mAb 11D5 anti-opsin COOH-terminal and mAb E anti-opsin NH_2-terminal. Diagram shows cleavage sites after limited thermolytic digestion of the membrane-bound bovine rhodopsin (Hargrave et al., 1987), as well as mAb 11D5 and mAb E binding sites. After digestion, opsin is cleaved to smaller fragments of ~32 and 26 kD in both membrane populations. Undigested opsin and its 69-kD dimer are reactive with both antibodies. The digested fragments are reactive only with mAb E, indicating that the COOH-terminal domain has been destroyed by proteolysis at the cytoplasmic surface of the membrane.

shown in Fig. 9. Binding of this antibody to ELISA plates coated with bovine opsin was inhibited by the synthetic peptide corresponding to the 1′–9′ (COOH-terminal) sequence of bovine opsin, with the concentration for 50% inhibition (IC_{50}) of 0.1 nM (Adamus, G., and P. Hargrave, personal communication). Although, mAb 11D5 is found to be specific for opsin, if the gel is overloaded with fraction 5 membranes it also binds to a 20-kD peptide (this specificity persists despite subcloning twice). mAb 11D5 labels ROS disk and plasma membrane and vesicles clustered near the cilium in the inner segment on thin sections of frog retinas, as shown in Fig. 10, in a pattern comparable to prior immunoelectron microscopic studies of retinas which were labeled with anti-opsin antibodies (Papermaster et al., 1985).

Immunoisolation of the Opsin-bearing Transport Vesicles

Opsin-bearing vesicles were isolated from fraction 5 by adsorption of membranes to beads coated with mAb 11D5. Electron microscopy shows that bound vesicles decorated the antibody coated beads (Fig. 11 *A*), while no membranes were attached to the beads coated with non-specific murine IgG1 (data not shown). Vesicles bound to 11D5 immunobeads appear to be smaller than fraction 5 vesicles shown in Fig. 8. However, examination of the large number of beads with bound vesicles suggests that there are also larger vesicles attached to the beads, but they often collapse, probably as a consequence of the treatment during immunoisolation. Moreover, ~85% of the radiolabeled fraction 5 membrane proteins are bound after incubation with the mAb 11D5 coated beads, suggesting that the majority of the fraction 5 membranes are immunoisolated with this antibody. Only ~10% of radiolabeled proteins are nonspecifically adsorbed by the control IgG1 coated immunobeads. Autoradiograms of radiolabeled membranes that are immunoisolated with mAb 11D5 coated beads, separated by SDS-PAGE and blotted onto Immobilon-P membranes are shown on Fig. 11 *B*. Antibody coated beads adsorb the majority of the sedimentable radiolabeled membranes regardless of the starting material: either total fraction 5 from the sucrose gradient, or the 40,000 rpm pellet of fraction 5. Total fraction 5 contains proteins that are not sedimentable after dilution with 10 mM Tris and are not adsorbed to the mAb 11D5 coated beads. Their cosedimentation with fraction 5 membranes into the initial gradients and their release into the supernatant of diluted and pelleted fraction 5 membranes suggests that they are peripheral membrane proteins. The specificity of their association with the membranes is under further study. Membrane proteins specifically bound to mAb 11D5 coated beads have the same relatively simple pattern described earlier in the high speed pellet of fraction 5 (c.f. Fig. 3 *B*). However, since protein content and exposure time of the autoradiograph shown on Fig. 3 *B* are >10 times higher than the one in Fig. 11 *B*, proteins other than opsin are not as readily detectable in Fig. 11 *B*. Presence of other membrane proteins of fraction 5 on the immunoisolated vesicles suggests that they may also be carried on the same vesicle as opsin and not on cosedimenting membranes.

Discussion

Post-Golgi membranes of frog retinal rods are an important contributor to the final structure of the cell since there is such a large amount of new ROS membrane generated each day. To ascertain their composition and to compare them to their counterparts in other highly polarized cells we isolated these membranes. To separate retinal subcellular organelles we found that shallow linear sucrose density gradients were valuable in partially attaining this goal. After newly synthesized opsin had left the Golgi apparatus and began to enter ROS, low density vesicles with a mean buoyant density of 1.09 g/ml became the most radiolabeled subcellular fraction. This buoyant density correlates well with the distribution of endocytic and exocytic vesicles described in other cells that are fractionated on similar sucrose density gradients (Mueller

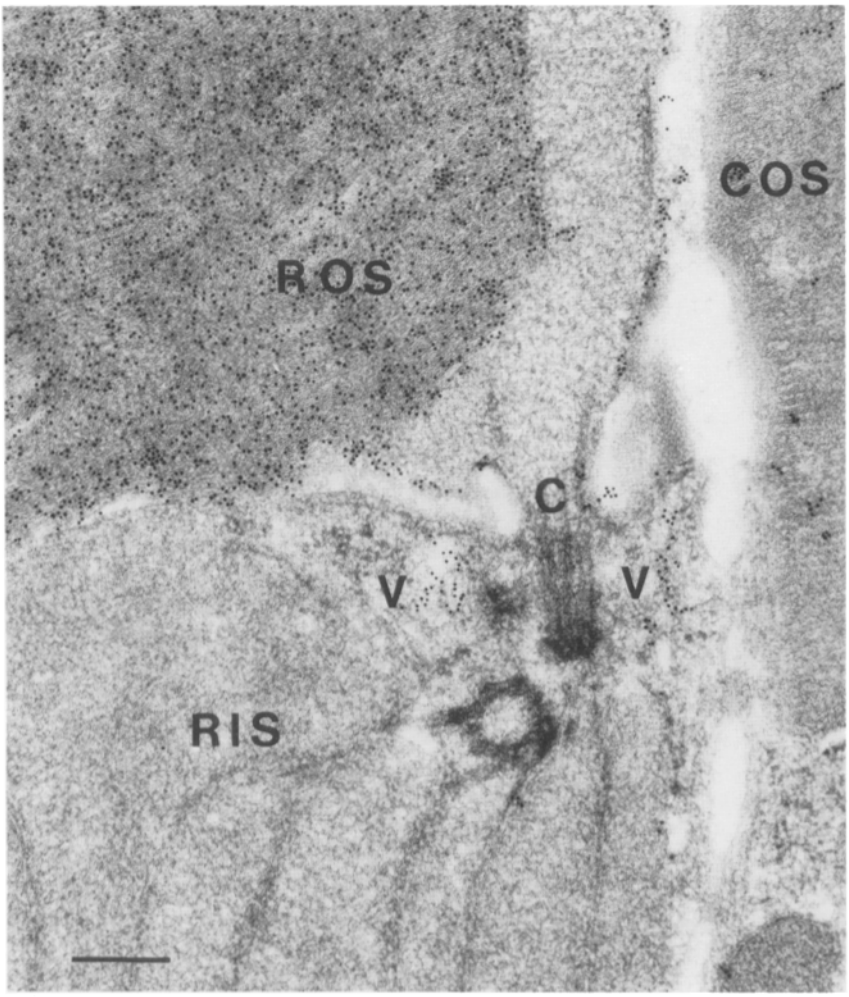

Figure 10. Monoclonal antibody 11D5 labels ROS disk and plasma membrane as well as transport vesicles clustered around the cilium on the thin section of the LR gold embedded frog retina. Plasma membrane of the rod inner segment is nearly unlabeled, as well as COS disk and plasma membranes. Bound mAb was detected with rabbit anti-mouse IgG followed by a goat anti-rabbit gold (10 nm) conjugate. *ROS*, rod outer segment; *COS*, cone outer segment; *C*, cilium; *V*, vesicles; *RIS*, rod inner segment. Bar, 0.3 μm.

and Hubbard, 1986; de Curtis and Simons, 1989). Although a low density vesicular fraction has also been reported as a pre-Golgi transport intermediate (Urbani and Simoni, 1990; Lodish et al., 1987), the kinetics of appearance of radiolabeled opsin in fraction 5, as well as the apparent molecular weight of mature opsin in its membranes, indicate that fraction 5 is largely a post-Golgi compartment.

Vesicles clustered beneath the connecting cilium have about 50% of the intramembranous particle (IMP) density of ROS disks when IMPs are quantitated in freeze-fracture EM studies (Besharse and Pfenninger, 1980) suggesting that these vesicles have a lower protein content and higher lipid/protein ratio than outer segment disks. Such vesicles should distribute into density gradient fractions that are lighter than outer segment disks, which sediment at ~1.12–1.13 g/ml (corresponding to fractions 7 and 8). The density of 1.09 g/ml for post-Golgi vesicles (fraction 5) is compatible with the expected density from the freeze fracture EM study.

Accumulation of newly synthesized opsin in fraction 5 vesicles simultaneously with its appearance in the ROS can also be explained by alternative possibilities: (*a*) fraction 5 contains endocytic vesicles, which are taking up newly synthesized opsin after its insertion into the plasma membrane or, (*b*) fraction 5 contains basal ROS disks, which are rich in newly synthesized opsin and have a different lipid/protein ratio that separates them from the older disks after homogenization and sedimentation on the sucrose gradients. Endocytic vesicles have been demonstrated in frog photoreceptor cells to function in the uptake of interphotoreceptor retinol binding protein (Hollyfield and Rayborn, 1987). If vesicles sedimenting in fraction 5 are generated by endocytosis, opsin would have to be inserted, at least transiently, into the inner segment plasma membrane. Very little immunocytochemically detectable opsin is found in the inner segment plasmalemma of amphibian rods (Besharse and Pfenninger, 1980; Nir and Papermaster, 1983) except near the periciliary ridge complex, a small area surrounding the cilium, where the transport vesicles fuse and deliver newly synthesized opsin (Peters et al., 1983; Papermaster et al., 1985, 1986). This is also shown in Fig. 10. Endocytosis of newly synthesized opsin from the plasma membrane is, therefore, a relatively unlikely source of the vesicles in fraction 5. However a transient source on the inner segment plasma membrane could be missed by EM techniques, if a small fraction of newly synthesized opsin chains is sorted by transcytosis, an additional sorting step suggested by Matter et al. (1990). Our studies do not exclude the possibility that transcytosis might be used if there are missorted proteins in the photoreceptor cell.

Nearly all of the ROS membranes are removed from the

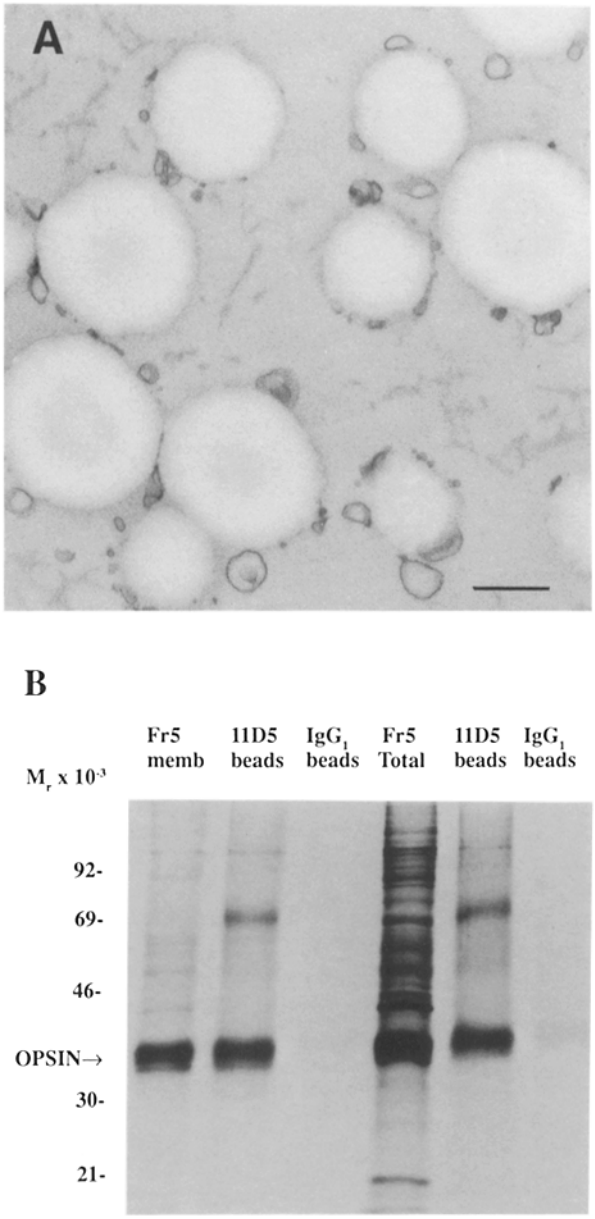

Figure 11. Vesicles from the gradient fraction 5 may be immunoisolated with the beads coated with mAb 11D5. (*A*) Electron microscopy of the vesicles adsorbed on beads coated with mAb 11D5, after incubation with gradient fraction 5. (*B*) Autoradiogram of radiolabeled membrane proteins bound to the beads separated by SDS-PAGE and blotted onto Immobilon-P membranes. When immunobeads were incubated with the membranes pelleted from fraction 5 (lane *1*), or with the total fraction from the sucrose gradient (lane *4*), the composition of radiolabeled material bound to mAb 11D5-coated beads (lanes *2* and *5*) or murine IgGl-coated beads (lanes *3* and *6*) did not change. Immunoisolated membranes appear to contain more opsin 69-kD dimer than the starting material, probably because of the prolonged treatment of the membranes before solubilization which promotes aggregation. Only freshly solubilized membranes contain no opsin dimer on the SDS gels. Aliquots in each lane equal ~0.2 retinas. Radiolabeled membranes shown in lane *5* here correspond to the sample analyzed by electron microscopy (*A*). Bar, 0.5 μm.

remainder of the retina during the first low-shear homogenization step, but each preparation of subcellular fractions from the rest of the retina still has ~3% ROS contamination. As shown in Fig. 3 *A*, the amount of the residual ROS from six retinas that sediment in fractions 7 and 8 is comparable to the amount isolated from 0.2 retinas. There is a possibility that contaminating radiolabeled ROS disks can separate into two fractions after homogenization: one that sediments in fractions 7 and 8 and is relatively unlabeled, and another that sediments in lighter fractions and contains only newly synthesized basal ROS disks. If vesiculated basal disks are the source of radiolabeled opsin in fraction 5, a certain portion of those disks should also be removed from the retina after the ROS separation and should appear simultaneously in the isolated ROS. We evaluated the kinetic order in which fraction 5 and ROS compartments acquire radiolabeled opsin when we perturbed intracellular transport with BFA, a drug that reversibly blocks transport out of, but not back to, the ER. When we included BFA in the retinal incubation media, opsin transport was reversibly inhibited; upon removal of the drug, newly synthesized opsin failed to reach outer segments after 2 h of chase but did reenter the post-Golgi vesicles in fraction 5. This provides evidence that fraction 5 membranes are not derived from highly labeled basal ROS disks. The reappearance of radiolabeled opsin in the membranes of fraction 5 after release from BFA inhibition indicates that the radiolabeled vesicles are exocytic post-Golgi carriers.

Formation of an extended Golgi-ER compartment by the action of BFA that is added only during the chase significantly inhibited opsin accumulation in the post-Golgi vesicles, but did not influence post-Golgi transport of newly synthesized opsin molecules that had already passed the barrier created by the drug. It is interesting to note that addition of BFA only during the chase period (30 min or 2 h) caused appearance of more slowly migrating (untrimmed) forms of opsin in fractions 9–14, while in the prolonged, constant presence of the drug (nearly 4.5 h of preincubation, incubation, and chase), opsin was modified to a more rapidly migrating form by oligosaccharide processing enzymes which were probably redistributed to the merged Golgi-ER compartment, as suggested by Ulmer and Palade (1989).

We have used monoclonal antibodies for immunoisolation of fraction 5 membranes; one of these, mAb 11D5, reacts avidly with opsin's COOH-terminal domain. The majority of sedimentable radiolabeled membrane proteins in this fraction appeared in the immunoisolated membranes using this mAb, which indicates that they are associated with opsin-bearing vesicles. The protein content of these vesicles is extremely simple compared to all other retinal subcellular fractions except for the ROS. Exocytic vesicles of BHK cells are also simpler in composition compared to Golgi and ER fractions (de Curtis and Simons, 1989).

It still remains to be determined if opsin or any of its associated proteins provide the vesicles with the necessary sorting information to direct them to the base of the connecting cilium and to avoid fusion with the lateral cell membranes or transport along the axon to the synapse. Expression of opsin in transfected polarized kidney epithelial cells leads to its accumulation in the plasma membrane but its distribution is not polarized (Oprian et al., 1987; Nathans et al., 1989). An additional signal may therefore be needed for localized delivery to and/or restriction of randomization from special do-

mains such as the outer segment in the frog rod. In preliminary studies we have identified, on blots of the SDS gels of the vesicle fraction, three low molecular mass GTP-binding proteins (M_r = 21–25 kD) and a smaller 20-kD protein (p20) whose functions in the rod cells are unknown. Similar GTP-binding proteins were demonstrated as components of transport vesicles in yeast (Salminen and Novick, 1987; Walworth et al., 1989) and were localized to specific exocytic and endocytic compartments in mammalian cells (Chavrier et al., 1990). The 20-kD protein (p20) is prominently labeled after [^{35}S]methionine incorporation and does not bind GTP. We have obtained a partial amino acid sequence of p20 and found that it is highly homologous and immunologically related to lens αB-crystallin (Deretic, D., R. Aebersold, and D. S. Papermaster, manuscript in preparation). Other proteins present in fraction 5 include G-protein (transducin) and cGMP phosphodiesterase which function primarily in the ROS, and β-tubulin.

Microtubules appear not to be involved in the transport of opsin through the mitochondria-rich ellipsoid region at the apex of the frog rod inner segment because its transport to the ROS is not inhibited by nocodazole (Vaughan et al., 1989). Which cytoskeletal elements, if any, are used for the transport of opsin remains unknown.

Newly synthesized proteins destined for the rod outer segment may move vectorially along a continuous reticulum where "vesicles" are actually discrete swellings along the reticular cisternae. Such a reticulum has been described in the endocytic pathway of epidermoid cancer (Hep-2) cells (Hopkins et al., 1990) and the *trans*-Golgi reticulum of astrocytes (Cooper et al., 1990). At the base of the connecting cilium in the photoreceptor, the juxtaciliary membranes appear to be 100-nm-diam vesicles (Papermaster et al., 1985, 1986) while the vesicles we have isolated are considerably larger and are comparable in size to the "varicosities" of the reticulum described by Hopkins et al. (1990). Isolation and characterization of these membranes and evaluation of their kinetics of transport are simply the first steps toward clarifying these issues. If some of the molecules that are associated with the opsin-bearing transport membranes are generally used by other polarized cells, the study of this unusual neuron will have a more general impact on the exploration of the problem of attainment and maintenance of cell polarity.

We thank Nancy Ransom for her expert electron microscopy; Cynthia McKee, Peggy Miller, Andrea Tate, and Tammy Lowe for their assistance; and Drs. Barbara Schneider, Kai Simons, Ann Hubbard, Hans-Peter Hauri, Heidi Hamm, Izhak Nir, and Neeraj Agarwal for helpful discussions. We also thank Drs. Patricia Cameron, Pietro DeCamilli, and Reinhard Jahn for immunobead methods, Drs. Hamm, Mangini, Molday, Valtorta, and Mercer for antibodies, and Drs. Adamus and Hargrave for assays of the specificity of mAb 11D5.

Supported by National Institutes of Health grant EY-6891.

Received for publication 9 October 1990 and in revised form 8 February 1991.

References

Adamus, G., A. Arendt, P. A. Hargrave, R. Jackson, J. H. McDowell, A. Szary, and H. E. Hamm. 1985. Use of synthetic peptides to evaluate cross-reactivity of monoclonal antibodies raised against frog rhodopsin. *In* Peptides: Structure and Function. C. M. Deber, V. J. Hrudy and K. D. Kopple Pierce, editors. Pierce Chemical Co., Rockford, IL. 55–58.

Balch, W. E., W. G. Dunphy, W. A. Braell, and J. E. Rothman. 1984. Reconstitution of the transport of protein between successive compartments of the Golgi measured by the coupled incorporation of *N*-acetylglucosamine. *Cell.* 39:405–416.

Bartles, J. R., H. M. Feracci, B. Stieger, and A. L. Hubbard. 1987. Biogenesis of the rat hepatocyte plasma membrane in vivo: comparison of the pathways taken by apical and basolateral proteins using subcellular fractionation. *J. Cell Biol.* 105:1241–1251.

Bennett, M. K., A. Wandinger-Ness, and K. Simons. 1988. Release of putative exocytic transport vesicles from perforated MDCK cells. *EMBO (Eur. Mol. Biol. Organ.) J.* 7:4075–4085.

Berryman, M. A., and R. D. Rodewald. 1990. An enhanced method for post-embedding immunocytochemical staining which preserves cell membranes. *J. Histochem. Cytochem.* 38:159–170.

Besharse, J. C. 1986. Photosensitive membrane turnover: differentiated membrane domains and cell-cell interaction. *In* The Retina: A Model for Cell Biological Studies. R. Adler and D. Farber, editors. Academic Press, Inc., New York. 297–352.

Besharse, J. C., and K. H. Pfenninger. 1980. Membrane assembly in retinal photoreceptors. I. Freeze-fracture analysis of cytoplasmic vesicles in relationship to disc assembly. *J. Cell Biol.* 87:451–463.

Burger, P. M., E. Mehl, P. L. Cameron, P. R. Maycox, M. Baumert, F. Lottspeich, P. DeCamilli, and R. Jahn. 1989. Synaptic vesicles immunoisolated from rat cerebral cortex contain high levels of glutamate. *Neuron.* 3:715–720.

Chavrier, P., R. G. Parton, H.-P. Hauri, K. Simons, and M. Zerial. 1990. Localization of low molecular weight GTP binding proteins to exocytic and endocytic compartments. *Cell.* 62:317–329.

Cooper, M. S., A. H. Cornell-Bell, A Chernjavsky, J. W. Dani, and S. J. Smith. 1990. Tubulovesicular processes emerge from *trans*-Golgi cisternae, extend along microtubules, and interlink adjacent *trans*-Golgi elements into a reticulum. *Cell.* 61:135–145.

De Camilli, P., S. M. Harris, B. Huttner, and P. Greengard. 1983. Synapsin I (Protein I), a nerve terminal-specific phosphoprotein. II. Its specific association with synaptic vesicles demonstrated by immunocytochemistry in agarose-embedded synaptosomes. *J. Cell Biol.* 96:1355–1373.

de Curtis, I., and K. Simons. 1989. Isolation of exocytic carrier vesicles from BHK cells. *Cell.* 58:719–727.

Defoe, D. M., and J. C. Besharse. 1985. Membrane assembly in retinal photoreceptors. II. Immunocytochemical analysis of freeze-fractured rod photoreceptor membranes using anti-opsin antibodies. *J. Neurosci.* 5:1023–1034.

Deretic, D., and H. E. Hamm. 1987. Topographic analysis of antigenic determinants recognized by monoclonal antibodies to the photoreceptor guanyl nucleotide-binding protein, transducin. *J. Biol. Chem.* 262:10839–10847.

Dunn, W. A., and A. L. Hubbard. 1984. Receptor-mediated endocytosis of epidermal growth factor by hepatocytes in the perfused rat liver: ligand and receptor dynamics. *J. Cell Biol.* 98:2148–2159.

Ey, P. L., S. J. Prowse, and C. R. Jenkin. 1978. Isolation of pure IgG_1, IgG_{2a} and IgG_{2b} immunoglobulins from mouse serum using protein A-Sepharose. *Immunochemistry.* 15:429–436.

Fanger, B. O. 1987. Adaptation of the Bradford Protein Assay to membrane-bound proteins by solubilizing in glucopyranoside detergents. *Anal. Biochem.* 162:11–17.

Fukuda, M. N., D. S. Papermaster, and P. A. Hargrave. 1979. Rhodopsin carbohydrate: structure of small oligosaccharides attached at two sites near the NH_2 terminus. *J. Biol. Chem.* 254:8201–8207.

Greenberger, L. M., and J. C. Besharse. 1983. Photoreceptor disc shedding in eye cups. *Invest. Ophthalmol. Vis. Sci.* 24:1456–1464.

Hall, M. O., D. Bok, and A. D. E. Bacharach. 1969. Biosynthesis and assembly of the rod outer segment membrane system. Formation and fate of visual pigment in the frog retina. *J. Mol. Biol.* 45:397–406.

Hargrave, P. A., J. H. McDowell, E. Smyk-Randall, E. D. Siemiatkowski-Juszczak, T. Cao, A. Arendt, and H. Kühn. 1987. Limited proteolysis of rhodopsin by thermolysin as a probe of protein structure and topography. *In* Membrane Proteins. S. C. Goheen, editor, Bio-Rad Laboratories, Gaithersburg, MD. 81–93.

Hollyfield, J. G., and M. E. Rayborn. 1987. Endocytosis in the inner segment of rod photoreceptors: analysis of *Xenopus laevis* retinas using horseradish peroxidase. *Exp. Eye Res.* 45:703–719.

Hopkins, C. R., A. Gibson, M. Shipman, and K. Miller. 1990. Movement of internalized ligand-receptor complexes along a continuous endosomal reticulum. *Nature (Lond.).* 346:335–339.

Kühn, H., O. Mommertz, and P. Hargrave. 1982. Light-dependent conformational change at rhodopsin's cytoplasmic surface detected by increased susceptibility to proteolysis. *Biochim. Biophys. Acta.* 679:95–100.

Kohler, G., and C. Milstein. 1975. Derivation of specific antibody producing tissue culture and tumor lines by cell fusion. *Eur. J. Immunol.* 6:511–519.

Laemmli, U. K. 1970. Cleavage of structural proteins during the assembly of the head of bacteriophage T4. *Nature (Lond.).* 227:680–685.

Liang, C.-J., K. Yamashita, H. Schichi, C. G. Mullenberg, and A. Kobata. 1979. Structure of the carbohydrate moiety of bovine rhodopsin. *J. Biol. Chem.* 254:6414–6418.

Lippincott-Schwartz, J., L. C. Yuan, J. S. Bonifacino, and R. D. Klausner. 1989. Rapid redistribution of Golgi proteins into the ER in cells treated with Brefeldin A: evidence for membrane cycling from Golgi to ER. *Cell.* 56:801–813.

Lippincott-Schwartz, J., J. G. Donaldson, A. Schweizer, E. G. Berger, H.-P. Hauri, L. C. Yuan, and R. D. Klausner. 1990. Microtubule-dependent retro-

grade transport of proteins into the ER in the presence of Brefeldin A suggests an ER recycling pathway. *Cell.* 60:821–836.

Lodish, H. F., N. Kong. S. Hirani, and J. Rasmussen. 1987. A vesicular intermediate in the transport of hepatoma secretory proteins from the rough endoplasmic reticulum to the Golgi complex. *J. Cell Biol.* 104:221–230.

MacKenzie, D., A. Arendt, P. Hargrave, J. H. McDowell, and R. S. Molday. 1984. Localization of binding sites for carboxyl terminal specific anti-rhodopsin monoclonal antibodies using synthetic peptides. *Biochemistry.* 23:6544–6549.

Mangini, N. J., and D. R. Pepperberg. 1988. Immunolocalization of 48K in rod photoreceptors. *Invest. Ophthalmol. Vis. Sci.* 29:1221–1234.

Matsudaira, P. 1987. Sequence from picomole quantities of proteins electroblotted onto polyvinylidene difluoride membranes. *J. Biol. Chem.* 262: 10035–10038.

Matter, K., M. Brauchbar, K. Bucher, and H.-P. Hauri. 1990. Sorting of endogenous plasma membrane proteins occurs from two sites in cultured human intestinal epithelial cells (Caco-2). *Cell.* 60:429–437.

Melancon, P., B. S. Glick, V. Malhotra, P. J. Weidman. T. Serafini, M. L. Gleason, L. Orci, and J. E. Rothman. 1987. Involvement of GTP-binding "G" proteins in transport through the Golgi stack. *Cell.* 51:1053–1062.

Misumi, Y., Y. Misumi, K. Miki, A. Takatsuki, G. Tamura, and Y. Ikehara. 1986. Novel blockade by Brefeldin A of intracellular transport of secretory proteins in cultured rat hepatocytes. *J. Biol. Chem.* 261:11398–11403.

Mueller, S. C., and A. L. Hubbard. 1986. Receptor-mediated endocytosis of asialoglycoproteins by rat hepatocytes: receptor-positive and receptor-negative endosomes. *J. Cell Biol.* 102:932–942.

Nathans, J., C. J. Weitz, N. Agarwal, I. Nir, and D. S. Papermaster. 1989. Production of bovine rhodopsin by mammalian cell lines expressing cloned cDNA: spectrophotometry and subcellular localization. *Vision Res.* 29: 907–914.

Nir, I., and D. S. Papermaster. 1983. Differential distribution of opsin in the plasma membrane of frog photoreceptors. An immunocytochemical study. *Invest. Ophthalmol. Vis. Sci.* 24:868–878.

Oprian, D. D., R. S. Molday, R. J. Kaufman, and H. G. Khorana. 1987. Expression of a synthetic bovine rhodopsin gene in monkey kidney cells. *Proc. Natl. Acad. Sci. USA.* 84:8874–8878.

Orci, L., V. Malhotra, M. Amherdt, T. Serafini, and J. E. Rothman. 1989. Dissection of a single round of vesicular transport: sequential intermediates for intercisternal movement in the Golgi stack. *Cell.* 56:357–368.

Papermaster, D. S., and W. J. Dreyer. 1974. Rhodopsin content in the outer segment membranes of bovine and frog retinal rods. *Biochemistry.* 13:2438–2444.

Papermaster, D. S., C. A. Converse, and J. Siu. 1975. Membrane synthesis in the frog retina: opsin transport in the photoreceptor cell. *Biochemistry.* 14:1343–1352.

Papermaster, D. S., B. G. Schneider, and J. C. Besharse. 1985. Vesicular transport of newly synthesized opsin from the Golgi apparatus toward the rod outer segment. *Invest. Ophthalmol. Vis. Sci.* 26:1386–1404.

Papermaster, D. S., B. G. Schneider, D. Defoe, and J. C. Besharse. 1986. Biosynthesis and vectorial transport of opsin on vesicles in retinal rod photoreceptors. *J. Histochem. Cytochem.* 34:5–16.

Peters, K.-R., G. E. Palade, B. G. Schneider, and D. S. Papermaster. 1983. Fine structure of a periciliary ridge complex of frog retinal rod cells revealed by ultrahigh resolution scanning electron microscopy. *J. Cell Biol.* 96:265–276.

Rodriguez-Boulan, E., and W. J. Nelson. 1989. Morphogenesis of the polarized epithelial phenotype. *Science (Wash. DC).* 245:718–725.

Salminen, A., and P. J. Novick. 1987. A *ras*-like protein is required for a post-Golgi event in yeast secretion. *Cell.* 49:527–538.

Schmied, R., and E. Holtzman. 1989. Involvement of the Golgi apparatus in sorting of materials to opposite ends of frog rod retinal photoreceptors. *J. Neurobiol.* 20:115–138.

Schneider, B. G., and E. Kraig. 1990. Na,K-ATPase of the photoreceptor: selective expression of $\alpha 3$ and $\beta 2$ isoforms. *Exp. Eye Res.* 51:553–564.

Schneider, B. G., A. W. Shyjan, and R. Levenson. 1991. Co-localization and polarized distribution of Na,K-ATPase $\alpha 3$ and $\beta 2$ subunits in photoreceptor cells. *J. Histochem. Cytochem.* 39:507–517.

Ulmer, J. B., and G. E. Palade. 1989. Targeting and processing of glycophorins in murine erythroleukemia cells: use of brefeldin A as a perturbant of intracellular traffic. *Proc. Natl. Acad. Sci. USA.* 86:6992–6996.

Urbani, L., and R. D. Simoni. 1990. Cholesterol and vesicular stomatitis virus G protein take separate routes from the endoplasmic reticulum to the plasma membrane. *J. Biol. Chem.* 265:1919–1923.

Valtorta, F., R. Jahn, R. Fesce, P. Greengard, and B. Ceccarelli. 1988. Synaptophysin (p38) at the frog neuromuscular junction: its incorporation into the axolemma and recycling after intense quantal secretion. *J. Cell Biol.* 107:2717–2727.

Vaughan, D. K., S. K. Fisher, S. A. Bernstein, I. L. Hale, K. A. Linberg, and B. Matsumoto. 1989. Evidence that microtubules do not mediate opsin vesicle transport in photoreceptors. *J. Cell Biol.* 109:3053–3062.

Walworth, N. C., and P. J. Novick. 1987. Purification and characterization of constitutive secretory vesicles from yeast. *J. Cell Biol.* 105:163–174.

Walworth, N. C., B. Goud, A. K. Kabcenell, and P. J. Novick. 1989. Mutational analysis of *SEC4* suggests a cyclical mechanism for the regulation of vesicular traffic. *EMBO. (Eur. Mol. Biol. Organ.) J.* 8:1685–1693.

Wandinger-Ness, A., M. K. Bennet, C. Antony, and K. Simons. 1990. Distinct transport vesicles mediate delivery of plasma membrane proteins to the apical and basolateral domains of MDCK cells. *J. Cell Biol.* 111:987–1000.

Weibel, E. R. 1979. Stereological Methods, Vol. 1. Academic Press, Inc. New York.

Wolf, K., and M. C. Quimby. 1964. Amphibian cell culture: permanent cell line from the bullfrog (*Rana catesbeiana*). *Science (Wash. DC).* 144:1578–1580.

Young, R. W. 1976. Visual cells and the concept of renewal. *Invest. Ophthalmol. Vis. Sci.* 15:700–725.

Young, R. W., and B. Droz. 1968. The renewal of protein in retinal rods and cones. *J. Cell Biol.* 39:169–184.